A Fundamental Study of
Bulk, Layered, and Monolayers of Hybrid Perovskites

by

Omar Alenezi

A Thesis Presented in Partial Fulfillment
of the Requirements for the Degree
Master of Science

Approved July 2019 by the
Graduate Supervisory Committee:

Sefaattin Tongay, Co-Chair
Richard King, Co-Chair
Yu Yao

ARIZONA STATE UNIVERSITY

August 2019

ABSTRACT

A Fundamental study of bulk, layered, and monolayers bromide lead perovskites structural, optical, and electrical properties have been studied as thickness changes. X-Ray Diffraction (XRD) and Raman spectroscopy measures the structural parameter showing how the difference in the thicknesses changes the crystal structures through observing changes in average lattice constant, atomic spacing, and lattice vibrations.

Optical and electrical properties have also been studied mainly focusing on the thickness effect on different properties where the Photoluminescence (PL) and exciton binding energies show energy shift as thickness of the material changes. Temperature dependent PL has shown different characteristics when comparing methylammonium lead bromide ($MAPbBr_3$) to butylammonium lead bromide (BA_2PbBr_4) and comparing the two layered n=1 materials butylammonium lead bromide (BA_2PbBr_4) to butylammonium lead iodide (BA_2PbI_4). Time-resolved spectroscopy displays different lifetimes as thickness of bromide-based perovskite changes. Finally, thickness dependence (starting from monolayers) Kelvin Probe Force Microscopy (KPFM) of the layered materials BA_2PbBr_4, Butylammonium(methylammonium)lead bromide ($BA_2MAPb_2Br_7$), and molybdenum sulfide (MoS_2) were studied showing an exponential relation between the thickness of the materials and their surface potentials.

I dedicate this work to my parents and my wife, who encouraged and believed in me to pursue my dream

ACKNOWLEDGMENTS

I would like to express my gratitude to my wonderful advisor Professor Sefaattin Tongay for letting me join his team to work on a cutting-edge field. He was one of a kind not only because of how well he knows and explains the concepts of 2D materials, but also because of how assiduous he is in teaching every member of his team technical, soft, and mental skills needed to become successful scientists, joining his research team was the best academic decision I have made.

I also appreciate each of Dr. Tongay's team members' help and inspirations as friends and fellow researchers, each member impacted this project in a way and everyone helped whenever I needed them, and most of all, I truly enjoyed working with them.

TABLE OF CONTENTS

Page

CHAPTER Page

LIST OF FIGURES

FIGURE Page

FIGURE Page

FIGURE Page

1 INTRODUCTION

1.1 2D Materials

Graphene, mechanically exfoliated by 2010 Nobel Laureates in Physics Novoselov and Geim, was the first 2D material studied at a fundamental level leading to a scientific breakthrough in 2004. Different properties change when the material reaches single layer thickness due to structural and quantum effects making these kinds of materials attractive. Graphene shows extraordinary properties including excellent thermal conductivity (5000 $Wm^{-1}k^{-1}$)[21] and extremely high electron mobility (250,000 cm^2/Vs)[22], high Young's modulus (1 TPa)[23], high transparency (97.5%)[24] , and large surface area (2630 m^2/g)[25], which can be used in different areas including electronics, energy, coatings and sensors nicknaming graphene as the "wander material".[26]

After graphene's discovery, more 2D semiconductor materials are needed to be discovered due to graphene's lack of having band gap, therefore, more 2d and ultrathin (> 1 nm) materials are being explored and studied theoretically and experimentally. Many 2D materials have been theoretically explored including the elemental atomically thin layers (Xenes) and transitional metal chalcogenides (TMCs), but the main materials that are being excessively studied experimentally are graphene, hexagonal-Boron Nitride (h-BN), transitional metals dichalcogenides (TMDs), black phosphorous, and recently and layered organic-inorganic hybrid perovskites; these atomically thin materials show superb electrical, optical, magnetic, chemical and mechanical properties for applications in nanoelectronics, optoelectronics, energy, biomedical, and waste management.[6,26,27]. Layered perovskites have shown changes in optical and electrical properties even when its thickness is not ultrathin, making this material special.

1.2 Perovskite

Organic-Inorganic Hybrid Perovskite plays a major role in optoelectronic devices because of its excellent electrical with it being ambipolar material, having long diffusion length, and high mobility.[1] It also have a spectacular optical properties with near optimal bandgap, bandgap tunability, broad absorption, and high absorption coefficient, which makes the material a great optoelectronic device attracting scientists and industries.[1] Perovskite Solar Cell (PSC), was the focus of many engineering labs the past ten years; it gained its popularity by being the fastest material to achieve a high power conversion efficiency (PCE) of about 24.2% in only 10 years.[2]

What makes PSC really attractive is its properties and its ease of fabricating an efficient device at a low cost and time consumption. In fact, different American Chemical Society (ACS) journals were published targeting audiences with no/low lab experience teaching them to fabricate a 15% and >20% PCE devices with precise and easy to understand directions.[3-4] Advancing at a fast pace encourages more teams with different backgrounds to join the perovskite project accelerating the advancement of PSC and other perovskite-based devices, and moving to manufacturing phase faster. This will surely impact the world economy and environment because the price of PSC will be encouraging for consumers to switch to renewable energy.

LED and photodetectors are another list of perovskite list of applications. NIR, red, and green Perovskite LEDs have achieved high quantum efficiencies exceeding 20%, and scientists are focusing on achieving a high blue LED efficiency.[28-31] As for the photodetectors, the technology has advanced to have a micron scale turn on/off with

responsivity reaching 10^4 AW^{-1} for bulk perovskite and detectivity reaching above 10^{15} Jones for 2D perovskite.[32-33]

1.2.1 Crystal Structure

Perovskite is a material with a special crystal structure of ABX_3, A being a large monovalent cation (Methylammonium [MA] or Formamidinium [FA], Cesium [Cs]), B is a small divalent cation like Lead (Pb) or Tin (Sn), and X being a halogen (Iodine [I], Bromine [Br], Chlorine [Cl]) with the unit cell consisting of 4 BX_6 octahedra structures and an A atom in the center. [5]

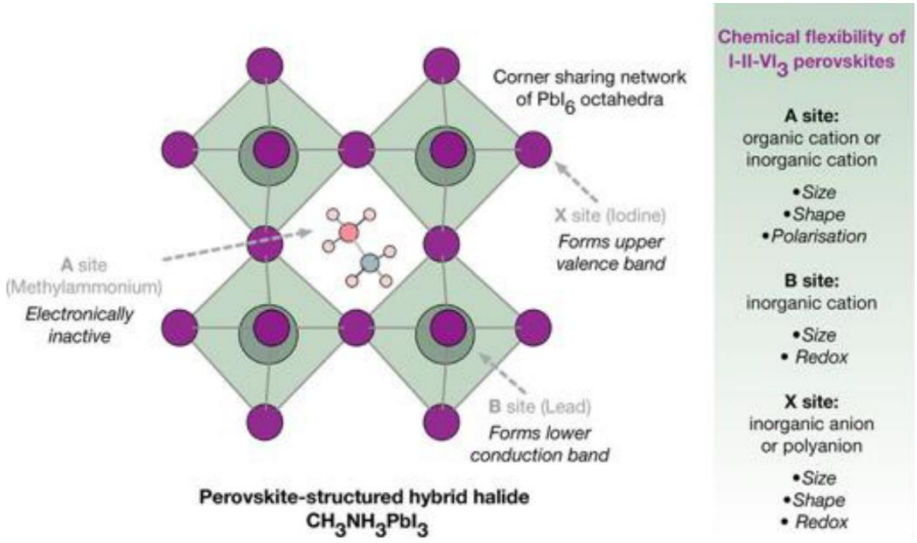

Figure 1. Schematic of $MAPbI_3$ crystal structure[F1]

The contribution of the A atom to the crystal structure is mainly formation and distortion of crystal structure.[5] these contributions can be estimated using Goldschmidt's Tolerance factor which states that tolerance T is proportional to the ionic radii of ions, which describes the distortion and stability of crystal structures, expressed as $T =$

$\frac{r_A+r_X}{[\sqrt{2}(r_B+r_X)]}$, r_A being the radius of the monovalent cation A, r_B is the radius of divalent cation B, and r_X is the radius of halogens X, showing that the larger r_A or the smaller r_B, the higher the tolerance factor until reaching the ideal factor 1 which is the cubic phase.

The material can change to one of three phases which are orthorhombic [γ], Tetragonal [β], and cubic [α]. These changes happen when the tolerance factor is not in the range of 0.85 – 1, where changing the phases affects the material properties. [5] Another factor that affects the phases is temperature which will be discussed in chapter 5. It is discussed that halogen affects the transition temperature of the three phases of perovskites, as halide's radius decreases the transition temperatures between perovskite phases decreases.[15] It is important because it shows that the cubic phase of Iodine-based perovskite (better absorption than other halogens) is unstable at room temperature, whereas Br-based and Cl-based perovskites are stable, so when creating mixed halide with iodine, cubic phase will become more stable opening a new opportunity of stability engineering. Another factor that impacts distortion is methylammonium spin, it has been mentioned that the dynamic of the bipolar monocation electrically distorts the BX octahedra.[16]

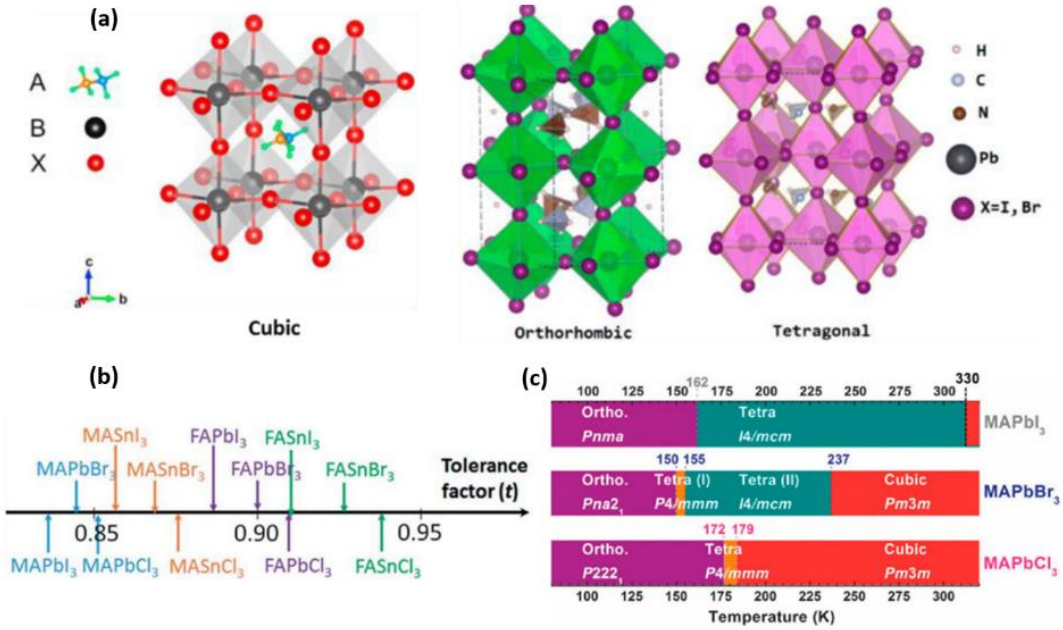

Figure 2. (a) Schematic of Cubic[F2], Orthorhombic[F3], and Tetragonal[F3] phases of $MAPbX_3$ crystal structures. (b) tolerance factors of different mixtures of A, B, and X[F4]. (c) Effect of Halogens on transition temperature between $MAPbX_3$ phases. [F5]

1.2.2 Electronic Structure

The octahedra structures determining the electronic properties of the perovskites. according to Yin *et al.*, Density Functional Theory - Perdew–Burke-Ernzerhof (DFT-PBE) has been used to calculate band structure and density of states (DOS) of $MAPbI_3$, the calculation shows that the material is direct bandgap and the conduction band minima (CBM) is determined from Pb 6p – I 5p π antibonding and Pb 6p – I 5s σ-antibonding with Pb 6p contributing the most while the valence band maxima (VBM) is determined from Pb 6s – I 5p σ-antibonding with Pb s being a lone pair instead of being empty s orbital attributing great electronic properties like high carrier mobility.[5, 14]

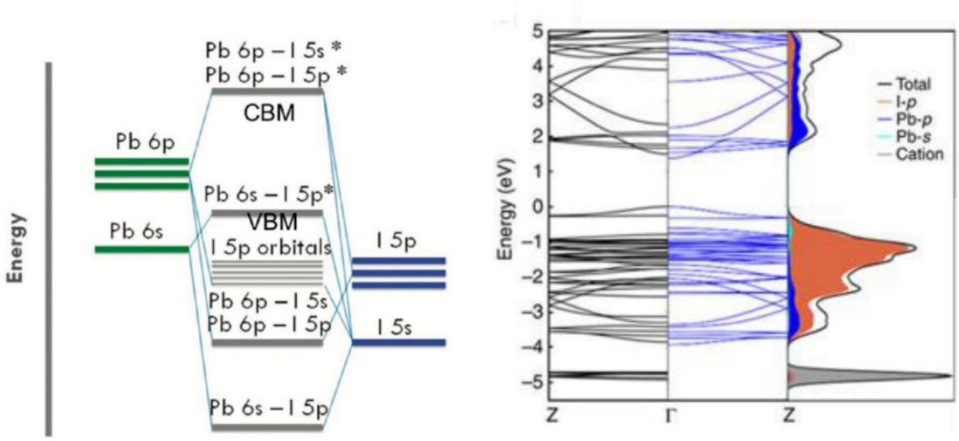

Figure 3. Left shows the DFT calculated Molecular Orbital Diagram of $MAPbI_3$.[F1] Right is the band structure and contributions of atoms of $MAPbI_3$.[F6]

Hybrid Perovskite is a direct band gap ranging from 2.3 eV – 3.1 eV depending on the halide used (increasing band gap when changing from I to Br and from Br to Cl as will be discussed in chapter 5). It also has a broad absorption spectrum and a high absorption coefficient.[1]

1.3 Layered Perovskite

Even though bulk perovskite has superior optical and electrical properties, the perovskite instability is a huge challenge, thus, layered perovskite has been seen as a good alternative to bulk perovskite because of its crystal structure, electrical and optical effects including dielectric separator, excitonic nature, and quantum confinement effects.[6]

1.3.1 Crystal Structure

The crystal structure of Ruddlesden-Popper 2D perovskites is $(R)_2(A)_{n-1}(B)_n(X)_{3n+1}$ (n=1,2,3, …,∞),[7] with R being a large aliphatic or aromatic alkylammonium organic cation spacer like Butylammonium [BA] or Phenylethylammonium [PEA] respectively, and n represents the number of layers before crystal is separated with the organic spacer.[8]

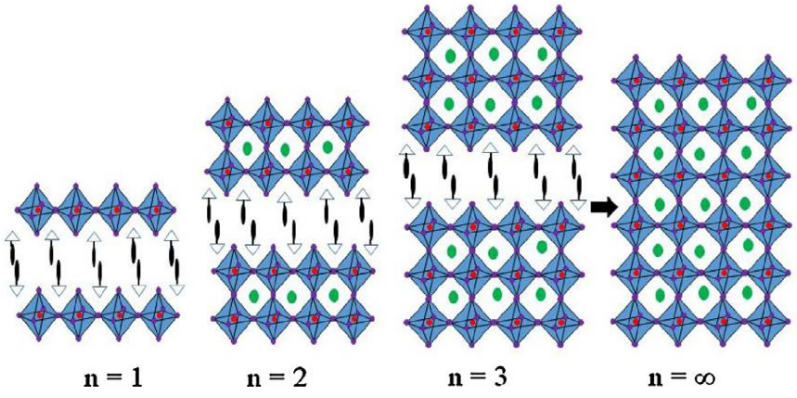

Figure 4. From left layered perovskite n=1, n=2, n=3, and n=∞ (bulk).[F7]

The nature of Ruddlesden-Popper perovskites crystal structure differs from that of the bulk perovskites crystal structure by having a large organic spacer between layers of BX_6 octahedra leading the force interaction between the layers to be van der Waals (vdW) thus the material changes from cubic structure to orthorhombic superlattice layered material.[6] One of the superb properties of layered perovskite is the ability to place the organic spacer after any number of BX_6 layers, for example at n = 1, the organic spacer is placed after every semiconducting layer, for n = 2, the spacer is placed after each two semiconducting, in fact studies have shown that the manipulation of n can reach 50, as such the spacer is placed after each n number of layers, which impacts the electrical and optical properties of the material.[33]

1.3.2 Electronic and Optical Properties

Electronic properties are determined mostly from the contribution of BX octahedra as discussed in section 1.1.3. But when the bulk changes to layered perovskite by adding organic spacer, it effects the electronic properties. The spacer causes the mobility to decrease since it acts as insulating layer; so, at n=1, even though stability greatly increases due to substituting out A atom like methylammonium and Formamidinium, insulating layer (BA, PEA) is added after every BX layer of the material significantly effecting electron mobility, thus it is not a good application for solar cell.[61] On the other hand, some teams suggested that the number of layers can be manipulated to increase the electron mobility by increasing n before adding insulating layer, n can exceed 10 or 100 like n = 50 greatly reducing the insulating effect of the organic spacer and achieving a good PCE (12%).[33] Major optical and electrical properties changes when perovskite becomes layered as will be discussed in chapter 5.

2 BACKGROUND AND CHALLENGES

2.1 Background

Advances of perovskite solar cell was astonishingly fast, encouraging different teams to join the perovskite project. Searching the term perovskite in google scholar resulted to more than 267,000 papers with 98,500 focusing on LED and 77,600 focusing on solar cell. Many teams got excited with perovskite recently, more so in solar cell and LED because in 2013 the solar cell device PCE surpassed 15% in just 4 years, and exceeded PCE of 24% in only 10 years opening number of new opportunities to expand and advance at a fast pace. Advancement in perovskite is quickly increasing with each year as new technologies and methods are being discovered and many theoretical concepts are being explained both of which lead to new questions and dig to deeper discoveries. Other perovskite optoelectronic devices that perovskite show tremendous potentials are LED with near infrared and green exceeding quantum efficiencies of 20% and photodetectors with a high on/off switch and detectivity.

Commercialization of perovskite devices has been the next focus since achieving high percentage of power conversion in different devices, but these devices face serious stability challenges including environmental (humidity and air), thermal, optical, electrical hysteresis, and lead poisoning due to many factors, which is why the trend shifted towards studying fundamentals of perovskite material and device stability, diverting the attentions to different research sub-areas.[1] The main sub-areas focused for research teams are studying and engineering monovalent cations, interface engineering, and passivation techniques. Industries will be encouraged to commercialize PSC when the device passes the International Electrotechnical Commission (IEC) 61646 for Thin

Film Modules standards, where it must survive a list of different types of accelerated aging tests including environmental, mechanical, and humidity stress tests for a long time (20 years for silicon standards).[13] Several teams broke the 10000 hours of instability barrier retaining 80% of the PCE but focusing only on parts of the accelerated aging test rather than applying all parameters (to mimic a harsh environment). So, from here on, two or more new stability challenges arise for the labs. The first is pushing the 10k hours barrier to 15k, 20k, or even 50k (depending on the advancement of stability topic) for specific aging tests. Another challenge is retaining >80% of the initial efficiency for 10k hours under all aging tests.

Methylammonium and Formamidinium were the first monovalent cations used in the fabrication of perovskite solar cell which succeeded in passing the 20% efficiency barrier, but the main problem is that both ions are organic which degrades perovskite material due to many stability factors. Instabilities have been studied individually to understand perovskite degradation mechanism. In the case of humidity, perovskite decomposes into MAI and BI_2 due to hydrolysis reaction.[18] As for the case of $MAPbI_3$ in the presence of dry O_2, the oxygen reacts with photoexcited electron generating superoxide (O_2^-), superoxide degrades the material to be PbI_2, I_2, CH_3NH_2, and H_2O.[19] Degradation due to thermal stability was studied to be found that the material has intrinsic thermal instability, which will degrade if the temperature reached 85 °C (environmental temperature is assumed 40 but temperature in device increases due to accumulation of heat in device).[20]

2.2 Challenges

Like every technology, there are many challenges that must be solved for the technology to proceed to the manufacturing phase. The main challenges that labs face in perovskite technologies are perovskite instabilities including organic instabilities (environmental air/humidity, thermal, and optical), electrical problems (hysteresis), and lead poisoning.[5] Many labs have succeeded with reducing the effects of the mentioned challenges by mixing different organic cations, alloying the cation metals, and mixing the halogens within the structure. Mixing organics mainly helps with crystal stability, example is a mixture between MA and FA (MA_xFA_{1-x}), or even mixing organic with inorganic materials like Cesium (Cs) and/or Rubidium (Rb) increasing the stability against air and humidity but instability is still a concerning issue even after applied mentioned solutions.[1]

Other initiatives shifted the focus towards 2D Ruddlesden-Popper hybrid perovskites to solve the instability challenge but faced electrical transport challenge due to the nature of the dielectric organic separator and absorption challenge. This challenge was faced by different solutions like manipulating the number of layers between the separator reaching the highest recorded of solar cell PCE of 13.7% and fabricating 2D/3D mixture (where $n \geq 20$) which reached 17.5%. Many labs focused more on devices and less on fundamentals, there are many unexplained and yet to be explored physics and chemistry of perovskites, some will be explained in this thesis.

3 SYNTHESIS AND CHARACTERIZATION

3.1 Synthesis:

Many methods can be used to synthesize perovskite material and generally each of the methods are used for specific goals; for example, anti-solvent crystallization is used to grow high quality single crystals,[11] sonicator is used to grow nanocrystals,[12] blade coating is used for materials roll-to-roll manufacturing, and spin coating is easy, cost and time effective. The time that takes the material to synthesize ranges from few minutes to several weeks depending on the method. This thesis will mainly focus on hybrid perovskite thin film and briefly mention single crystal, nanocrystals, and chemical vapor deposition for monolayer exfoliation and growth. It is strongly recommended for non-chemical engineers and scientists to get familiarized with molarity conversions for perovskites since it is not complex to synthesize, learning molarity conversions will give access to manipulating different organic/inorganic concentrations for bulk perovskites and different numbers of layers for layered perovskites where these manipulations play major roles in engineering different electrical and optical properties.

3.1.1 Spin-Coating

As briefly explained in chapter 1, many labs try to introduce a general, easy, and cost-effective method to fabricate Perovskite solar cell and LED. The techniques used by many teams which achieved a high efficiency of 24.2% for solar cell is spin-coating. Spin-coating is considered to be the simplest low-cost and time effective technique to grow solution-based materials to thin film.[9] The first step before depositing the material

in a spin-coater is to prepare the precursors, which consists of diluting the sample in a solvent and treating it, then depositing it on a substrate then spinning it.[9]

Thickness (t) of the film is determined based on spin speed (ω), viscosity, and surface tension, with $t \propto \frac{1}{\sqrt{\omega}}$, with a maximum variation of thin film factor of ~3.2 – If a thickness at a spin speed of 5000 rpm is 10 nm, then its thickness at around 500 rpm is 32 nm. [10] This technique can be used for organic and inorganic materials, metal precursors, metal oxides, photoresists, and many materials. [10] Disadvantages of spin-coating includes loss due to splash and hard to deposit large wafers.

This thesis will mainly focus on thin film fabrication method to measure many parameters. The reason that thin film is used as a sample of measurement because many hybrid perovskite optoelectronics devices have been fabricated using spin coating technique, while until recently, many fundamental studies of perovskite materials focus on high quality single crystal.

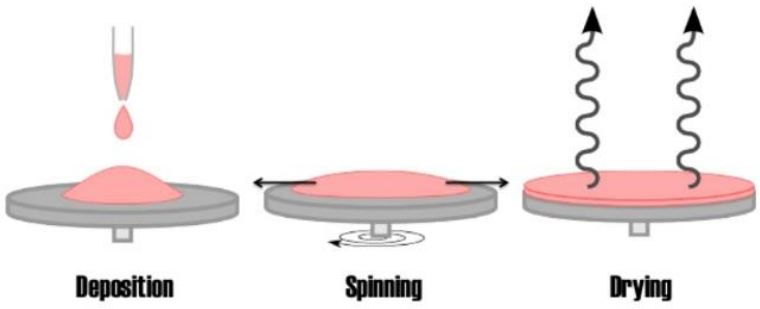

Figure 5. Diagram showing spin-coating steps and image of spin coater.[F8, F12]

3.1.2 Antisolvent Crystallization

Growing single crystal usually is for focusing on the crystal size and quality. It is a great method to better understand nucleation and crystallization of the material hence opening new opportunities in synthesis methodologies. Also, high quality single crystal is a perfect measurement sample for electrical, optical, mechanical, chemical, and magnetic properties to get better signals from different characterization methods. This method uses solvent that the solution scarcely dissolves (therefore antisolvent) to reach supersaturation, then nucleates and crystallizes if controlled the parameters like heat, time, and concentration properly.[35] single crystal can be used for mechanical exfoliation to get monolayers and ultrathin layers.

3.1.3 Chemical Vapor Deposition

CVD is an economic process that grows high quality crystals and thin films. CVD have several types each of which have different uses and advantages which are atmospheric pressure, low pressure, and plasma enhanced. The general process of CVD follows five steps starting with transport of the reactant to the substrate surface, adsorption of the reactant on the surface, reaction taking place, desorption of byproducts, and finally transport of byproduct from surface. CVD have many advantages including cost effective production-wise because of material forming together and below the melting point, flexibility with substrate shape, programing temperature profiles, and its versatility where any compound or element can be deposited.

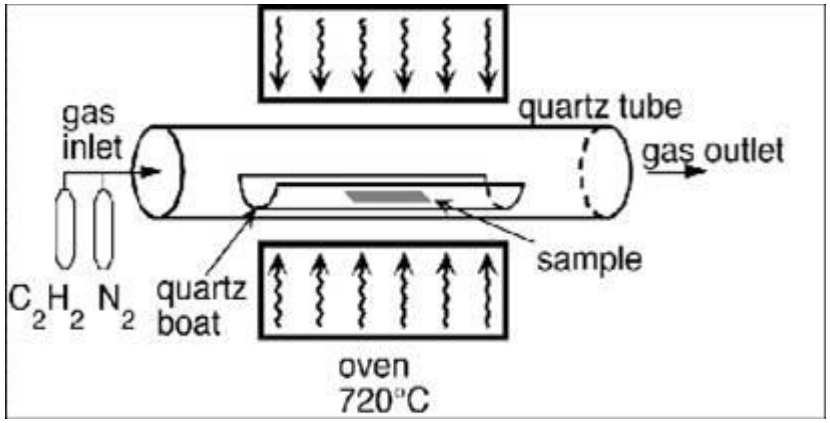

Figure 6. Diagram of CVD process.[F15]

Another advantage which can be a challenge is the number of parameters that should be accounted for the growth. It is an advantage because it gives a huge control over the growth environment, whereas it is considered challenging for synthesizing sensitive and unknown materials. Another disadvantage is constant cleaning of CVD tube and flow tubes to avoid defecting the sample.

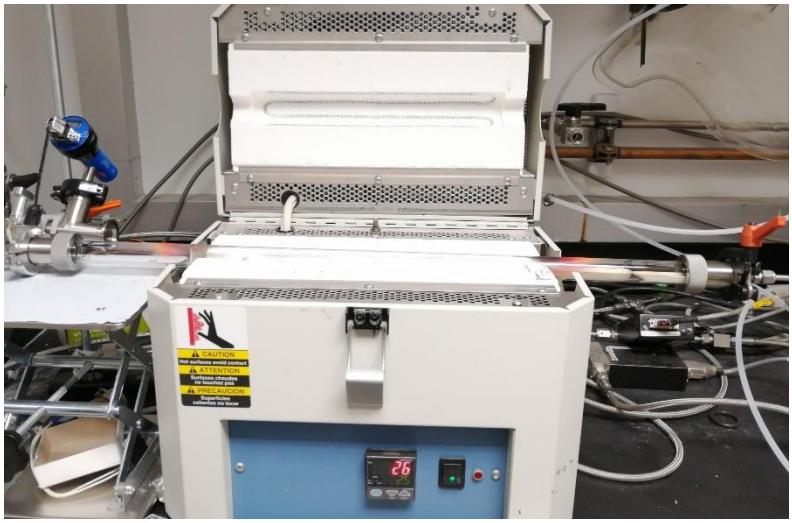

Figure 7. One of the lab's CVD furnaces.[F8]

3.2 Characterization

3.2.1 Raman Spectroscopy:

Raman spectroscopy is a non-destructive technique used to characterize the structure fingerprints of materials using monochromatic light – usually ranging from near IR to UV – used in wide range of fields including solid states and chemistry.

Figure 8. Raman Spectroscopy with light microscopy, blue laser, and UV laser source. On the right is inside the Raman with filters and lenses to increase emitted wavelength accuracy then read Raman scattered data.[F8]

After emitting energy, the detector observes different scatterings from the material. Coherent famously known as Rayleigh is a scattering that typically have the same wavelength as the incident beam. The second scattering is incoherent or Raman scattering (inelastic scattering) with wavelength that differs from the incident beam. Majority of the scattering is Rayleigh scattering and very small percentage is Raman, and the frequency difference observed between them is due to the vibration of the material. When the material gets excited, the absorbed energy is then re-emitted, if the re-emitted energy is less than the incident beam the phenomenon is called Stokes, if it re-emits more energy it is called Anti-Stokes.

The detector reads the vibration then calculates what wavenumbers the Raman peaks occur, the specific Raman peaks which is like fingerprints identifies the material and other peaks or shoulders of peaks indicates how defected the materials is.

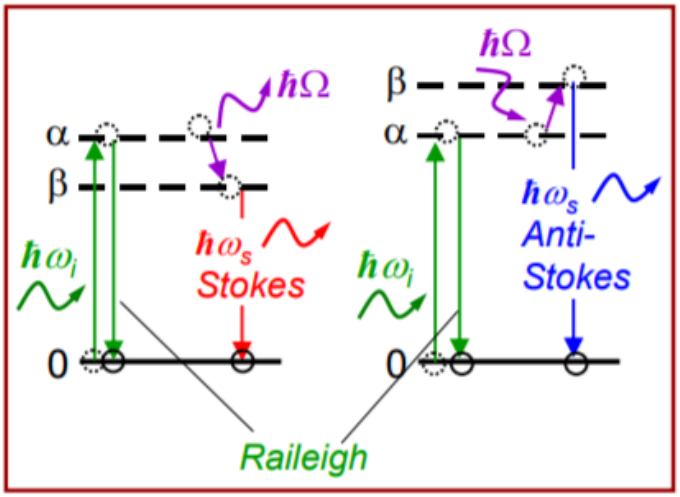

Figure 9. Left is Stoke and right is Anti-Stoke phenomena.[F9]

3.2.2 X-Ray Diffraction

XRD is another rapid and nondestructive technique used to study crystal structures. Instead of vibrations, this technique specializes in identifying the atomic spacing of crystals through emitting energy at a wavelength ranging 10 – 0.01 nm at different 2θ angle applying Bragg's Law. The law relates the atomic spacing with wavelength through diffraction angle as follows: $\lambda = 2dsin\theta$.

The diffraction is caused from the planes of crystal causing the incident X-rays to interfere with each other. Along with atomic spacing, XRD can be used to show crystal structure, spacing between layers, grain size, and orientation.

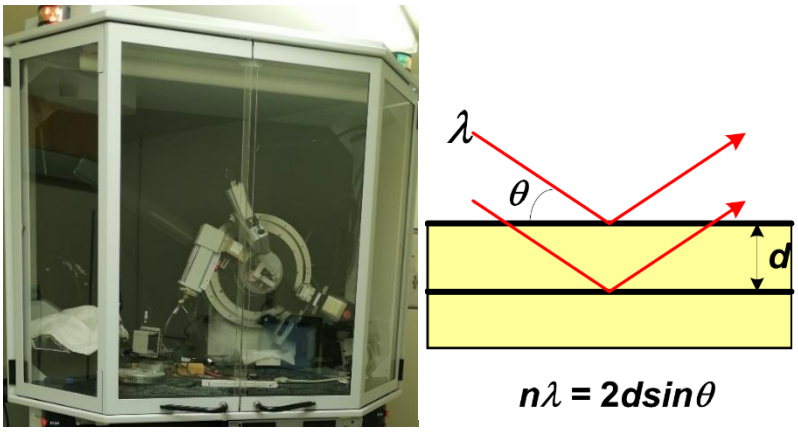

Figure 10. image of X-Ray Diffractometer and diagram of Bragg's Law.[F10-F11]

3.2.3 Atomic Force Microscopy

AFM is an excellent topography technique that scans the surface of a material with a nanoscale and angstrom resolution through a computer connected piezoelectric with microprobe tip at the head. The data is collected through passing a small current between the tip and the surface and when the tip is scanning the current causes a force which changes the oscillation of the cantilever which is sent as data. AFM can be used to scan flake thickness, manipulate atom positions, measuring surface potential, and many other applications.

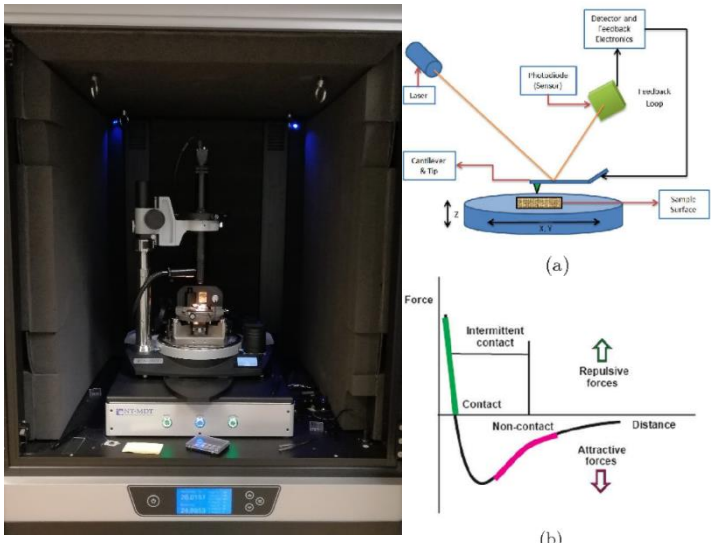

Figure 11. image, a) schematic of AFM, and b) graph of tip-sample surface force as a function of distance.[F8, F13]

3.2.3.1 KPFM

Kelvin Probe Force Microscopy is a tool used in AFM to image surface potential of materials at nano and subnano scale. The tool measures the potential difference between AFM tip and sample surface resulting in a map of surface potential. Knowing surface potential will directly lead to knowing the workfunction of the material – minimum amount of energy to remove an electron from a material surface to vacuum – through the equation $V = \frac{\Phi_{\mathrm{Tip}} - \Phi_{\mathrm{material}}}{-\mathrm{e}}$ where V is the surface potential between the tip and sample, Φ_{Tip} and Φ_{material} are the workfunctions of the tip and the material respectively, and e is electric charge.[38] Workfunction is a significant parameter for interface engineering of electronic and optoelectronic devices including Schottky Junction and tandem solar cells

3.2.4 Scanning Electron Microscopy

SEM is another topography technique which uses electron beam to study morphology, orientation of grains, grain size, thickness of the film, and other interesting parameters. It has high depth of focus and can achieve extremely high magnification (10^5) achieving nanometer resolution. Highly energized beam of electrons is generated from an electron gun under high vacuum scanning the surface using scanning coils. As the beam is scanning using pixel like technique, the sample produces secondary electrons showing the image of the loaded sample and the more secondary electrons are produced the higher the intensity of the pixel in an image.

Morphology, grain size, orientation of grains, and film thickness can be studied through the image. Chemistry of the material is analyzed using a detector called Energy Dispersive X-ray Spectroscopy (EDX/EDS) outputting different maps of elements and the elemental ratio in the material.

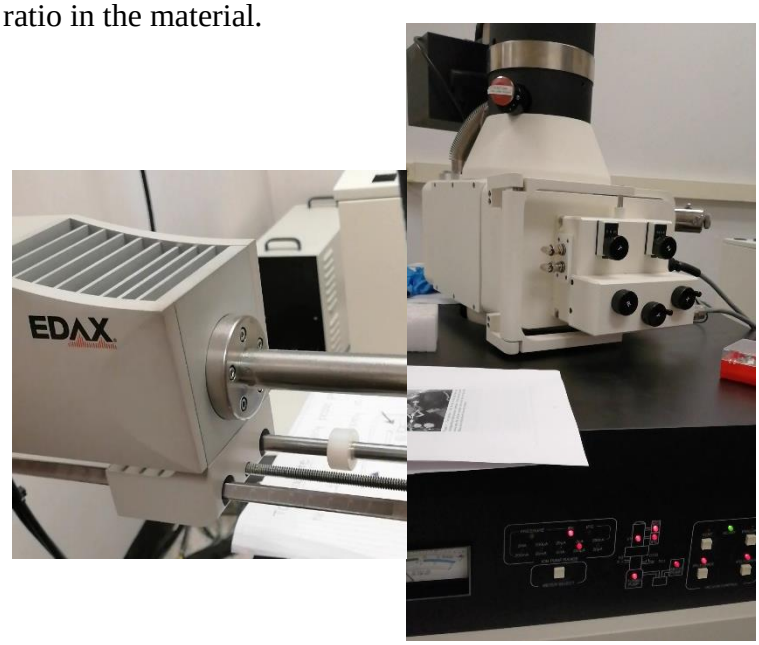

Figure 12. images of EDAX detector (left) and SEM (right).[16]

3.2.5 Photoluminescence

PL is a nondestructive technique that excites electrons of the material through light source, after picoseconds, electron recombines radiatively which then gets collected and computed, hence photo – luminescence. The excited electron is known as photoexcited electron, goes through either of the two dynamics, first is called Bimolecular process and second being monomolecular process.

In the Bimolecular process, hv (light) gets absorbed in the material – in the case of hv is $\geq$ than the band gap (hv slightly lower than band gap might get absorbed with the help of phonon) – creating electron-hole pair bound by Coulomb force called excitons. The photoexcited electron is excited to the conduction band leaving the holes in the valence band. Electrons and holes relax thermally almost immediately (10^{-15} s) to the CBM/VBM respectively through electron-phonon

(lattice vibration) interaction process called thermalization. The electron then recombines with hole radiatively emitting light, and non-radiatively emitting heat. The whole process normally takes nanoseconds unless the lifetime of the material is longer or enhanced.

Monomolecular process is the same up to the point of thermalization where the photoexcited electron and hole thermalize to trap under the CBM called bound state then recombines with hole emitting light and heat. The gap between the CBM and bound state is called exciton binding energy (E_b).

Sometimes E_b is very small (couple of meVs) that the Electronic band gap – the gap between excitons in bimolecular process – and the optical band gap – the gap between excitons in monomolecular process – is considered to be the same, hence PL in this case measures nonexcitonic materials' band gap. If the material is excitonic where the exciton binding energy is large, the PL can only measure the optical band gap. Generally, it is preferable to choose nonexcitonic materials for photovoltaic devices like solar cells and photodetectors while excitonic materials for emitting devices like LED and laser. In addition to band gap, PL can show defects, exciton states.

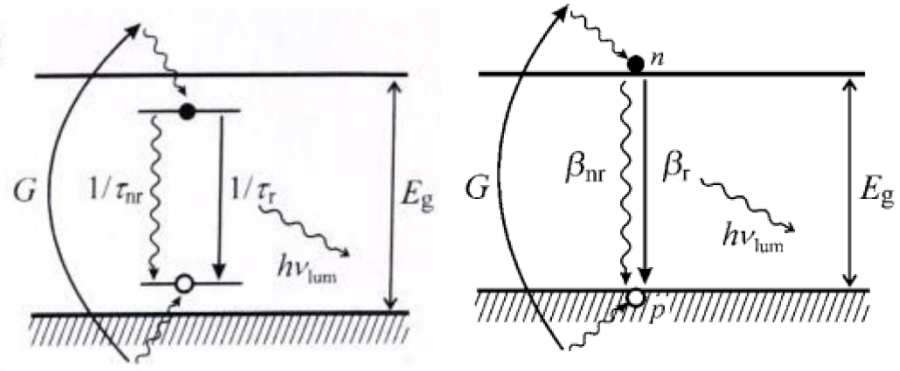

Figure 13. Diagrams of monomolecular and bimolecular processes.[F9]

3.2.5.1 Temperature-Dependence PL

Measurements at low temperature show many information which cannot be found or hard to find at room temperature the reason is some of the material parameters change and some phenomena appear while others disappear. Generally, phonon – electron interaction and electron – electron interaction decreases exponentially as temperature decreases due to losing energy, this results in getting signals easier and enhancing PL intensity, showing more accurate defect states, and the dynamics of different interactions. As temperature decreases another phenomenon plays a major role in shifting the energy, which is thermal expansion interaction, where the lattice constant of a material generally shrinks as the temperature decreases effecting the band structure of the material resulting in an increase in band gap. An empirical equation is used showing the effect of the temperature on a material's band gap called Varshni's empirical law and the relation is $E_g(T) = E(0) - \frac{\alpha T^2}{B+T}$, where $E(0)$ is the band gap of the material at 0 K and α and B are material constants.

Phonons (lattice vibration) gets altered from change of temperature resulting in the change of electronic band structure, where energy is inversely proportion to the exponential rate of phonon frequency ($E \propto \frac{1}{\exp(\omega)}$), and frequency is proportion to the spring constant K ($\omega^2 \propto K$). Therefore, increase in temperature decreases the spring constant resulting to decreasing the frequency of the lattice vibration, hence increases the band gap of the material.

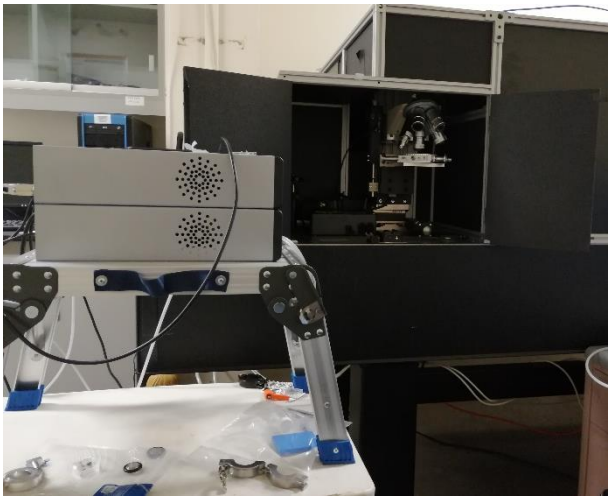

Figure 14. TDPL Setup.[F9]

3.2.5.2 Time-Resolved PL

TRPL is a strong technique that measures transport and recombination in semiconductors at picosecond scale through pulsing the laser then measuring the time difference between absorbance and transmittance. [34] The pulsed light excites the sample then the PL gets detected by a photodiode.[34] The main parameter that TRPL measures is the lifetime of the electron before it recombines. Lifetime is directly proportional to electrical conductivity of the material hence the higher the recombination lifetime the higher the conductivity becomes.

4 PEROVSKITES

The main perovskite material characterized in this thesis is methylammonium lead bromide ($MAPbBr_3$) because few labs focus on its fundamentals, second reason is that iodide-based material is more expensive and need to have storage system from light because iodine undergoes photo-decomposition as will explain in section 5.3.3.

4.1 Synthesis

As mentioned in section 4.1, there are many ways to synthesize perovskite materials, but this thesis will focus on two methods, thin film and anti-solvent crystallization. To prepare a solution, the chemistry must satisfy $MAPbBr_3$ material structure. As for thin films, the synthetization method is originated from ACS Chemical Education "Fabrication and Characterization of Perovskite Solar Cells- An Integrated Experience" paper.

Thin film is prepared using method called 1 step deposition. The 1 step deposition can be done by first dissolving 1 mmol of MABr in dimethylformamide (DMF) and mix it with 1 mmol of PbBr in DMF. If the materials are not available in the lab then the following reaction is a way to synthesize the reactants:

$$PbBr_2\text{: } 1\ mmol\ of\ PbO + 2\ mmol\ of\ HBr \rightarrow PbBr_2 + H_2O$$

$$MABr\text{: } 2\ mmol\ of\ CH_3NH_2\ (methylamine) + 2\ mmol\ of\ HBr \rightarrow 2CH_3NH_3Br\ (MABr)$$

Before deposition, the substrate must be thoroughly cleaned using Plasma cleaner or alcohols like IPA, ethanol, or both Plasma cleaner and alcohol depending on the substrate. For substrates like Indium Tin Oxide and Fluorine Tin Oxide, it is recommended to ultrasonicate using IPA, ethanol, then DI water for 5 minutes each, further clean it with Plasma Cleaner (Argon) for 15 minutes.[3]

To deposit the sample, the spin coater must be first programmed as follows: 500 rpm for 10 seconds, this is for depositing the solution while spinning at low speed; and the second program is 3000 rpm for 30 seconds, which spread the solution throughout the substrate creating uniformity. Next, transfer the substrate to a preheated hot plate at 100 150 °C immediately after the second program finishes, and leave for 20 minutes.

4.2 Raman Spectroscopy

Raman shows the fingerprints of the measured materials as discussed in section 4.2.1.1. The Raman spectroscopy of $MAPbBr_3$ shows three peaks in total, one peak is at sub 200 cm^{-1} and two peaks at 1350 and 1470 cm^{-1}. The peak is wide at low frequency with a shoulder probably due to defects, where it is shown in science advances that five peaks emerge when measuring low frequency at 80 K.[40] The Raman spectra at high frequency shows two peaks, both peaks shows in Xie *et al.* measurement but are shifted by ~ -100 cm^{-1}, where the published measurement show peaks at 1470 and 1545 cm^{-1} with a shoulder peak at 1614 cm^{-1}.

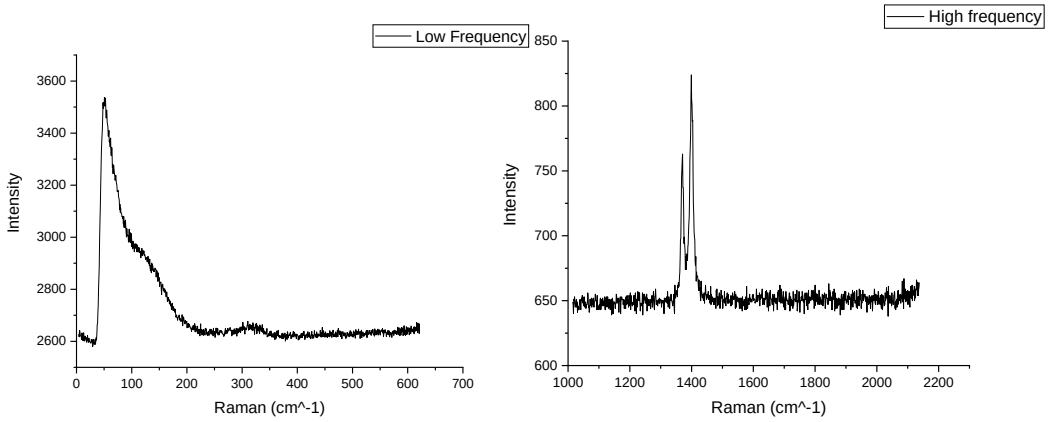

Figure 15. Raman Spectra at low and high frequency.

4.3 X-Ray Diffraction

XRD measurement is used to study crystal structure of $MAPbBr_3$. As discussed in section 1.2, the crystal structure of $MAPbBr_3$ at room temperature is cubic while the space group of $MAPbBr_3$ at room temperature is Pm3m according to Wang *et al.*[39] The X-Ray Diffraction spectrum of $MAPbBr_3$ shows peaks at 2θ= 15.07°, 29.2°, 30.07°, 46.02°, 47.28°, 48.1°, and 62.74 °which agrees with Wang *et al.* measurements. atomic spacings analysed through Jade ranges from 1.066 $\dot{A}$ – 1.537 $\dot{A}$ and the average lattice constant has been calculated to be 6 $\dot{A}$.

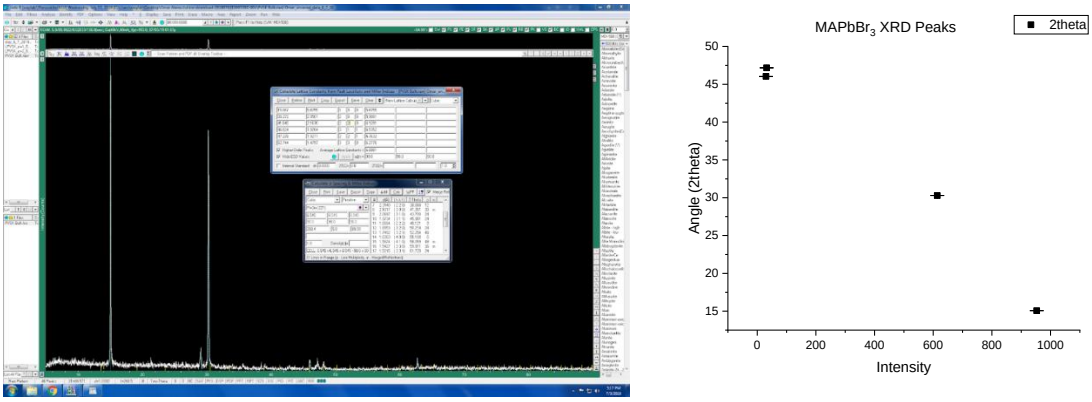

Figure 16. XRD Spectra of $MAPbBr_3$ with calculated atomic spacings and average lattice constant

4.4 Scanning Electron Microscopy

SEM was used to analyze the topography of $MAPbBr_3$ thin film. The film shows charged grains in the surface. The largest grains (5 – 10 μm) are shown as doughnut shaped and flower shaped and are outgrown out of the film as shown in the Figure 10 and film thickness is around 3.7 um and it shows that it is not layered. Also, grains show high electron charge around the edge while the middle is less electronically charged. It might be because it is because of the edge thickness being higher than the center thickness.

EDS Show the elements of the material except for hydrogen and nitrogen, Al is sapphire which mistakenly computed instead of bromine, Au is gold sputtering. The ratio between Pb and Br is approximately 1:3 which is the correct ratio of $MAPbBr_3$.

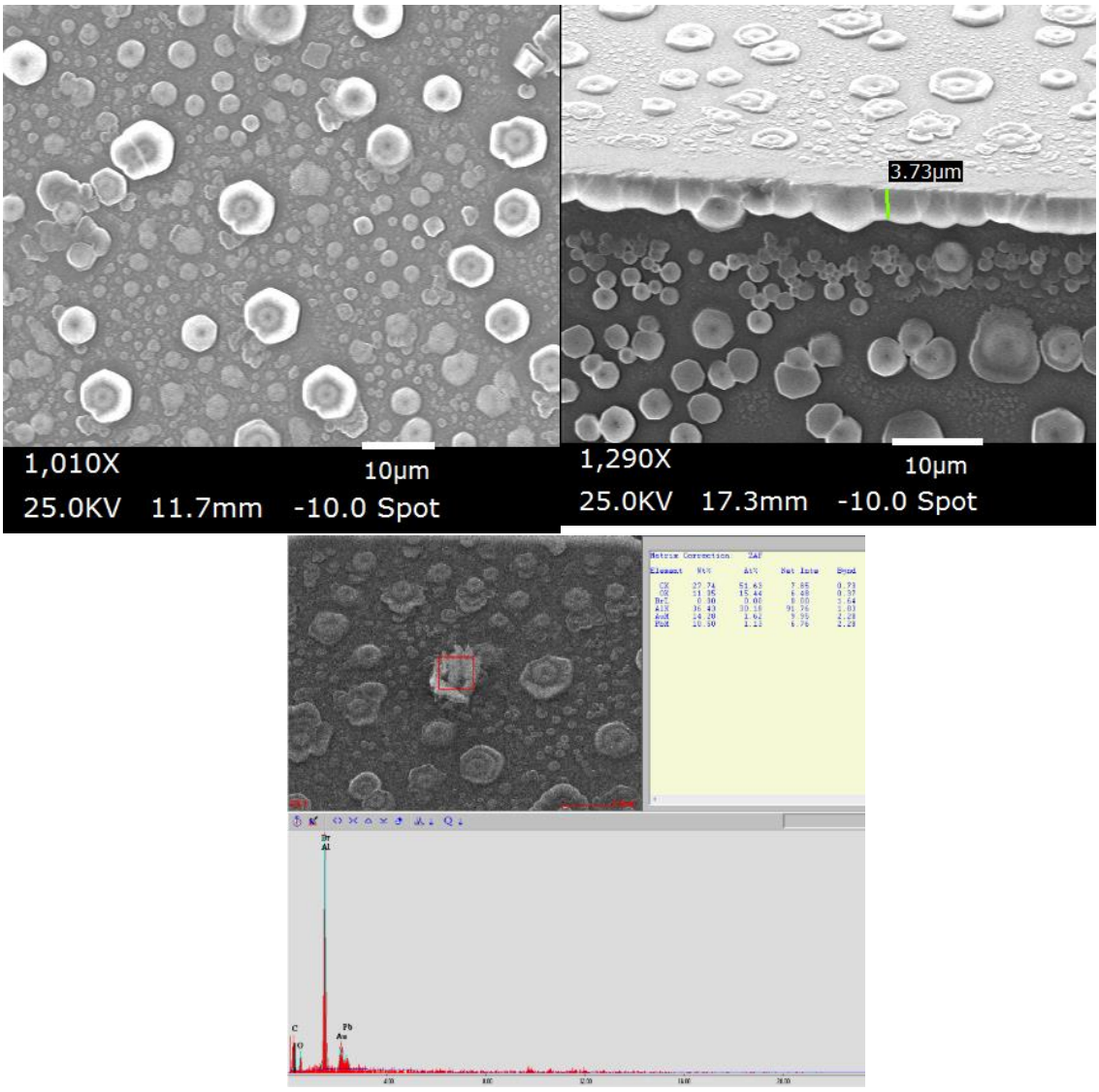

Figure 17. Top left and right images are top view and 40° angle view of $MAPbBr_3$ thin film on copper tape. Bottom middle is EDS chemistry analysis showing elements and weight% of elements in material.

4.5 Photoluminescence

The PL of $MAPbBr_3$ shows an optical band gap at ~2.308 eV. This shows that after absorption of energy, $MAPbBr_3$ emits energy at this level after nanoseconds, and this is due to the recombination effect, where after the material absorbs energy (hv), electron gets excited with enough energy to the conduction band, and after an amount of lifetime being free carrier, electron and hole recombine and emit energies in the form of heat and light, and such, the PL shows the radiated energy of the material.

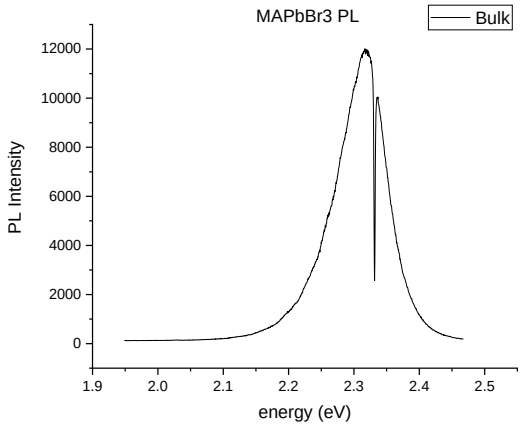

Figure 18. PL of $MAPbBr_3$.

4.5.1 Temperature-Dependent PL

TDPL is used to measure $MAPbBr_3$ band gap dependance on temperature. As mentioned in section 3.2.5.1, the band gap gets determined by the dominant parameter between thermal expansion interactiona and the phonon – electron interaction. TDPL has been taken with intervals of 10 K using green laser as excitation source for $MAPbBr_3$ microcrystals. The plot shows some PL peaks change from trend the which might be due to phase transition of the material.

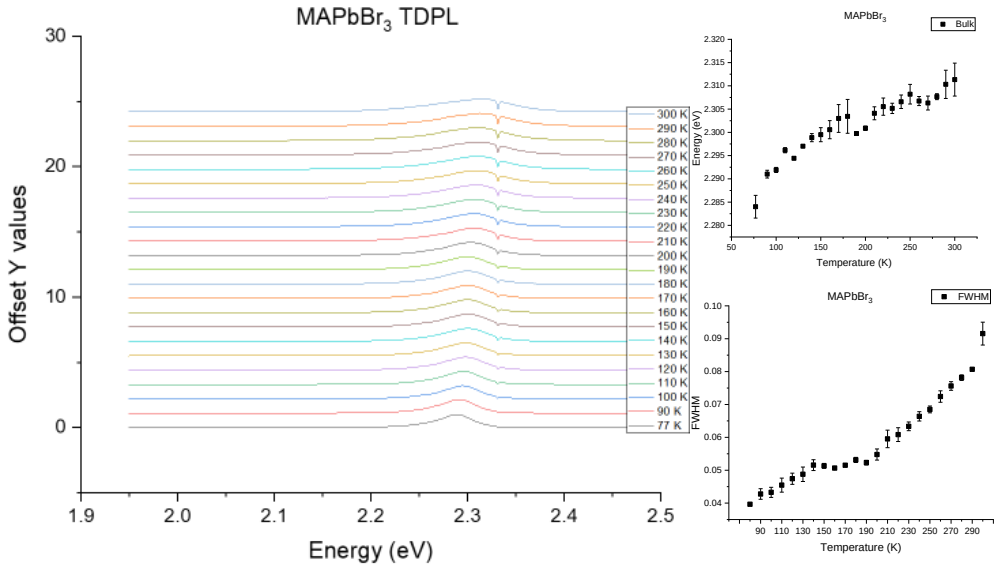

Figure 19. Top is TDPL of $MAPbBr_3$ with intervals of 10 K, bottom left is emission peaks with respect to temperature, and bottom right FWHM.

$MAPbBr_3$ shows a red shift of approximetly 25 meV meaning that the electron-phonon interaction is the dominant for $MAPbBr_3$, where the energy red shifts as temperature decreases due to increase in lattice vibration frequency.

5 LAYERED PEROVSKITES

Layered Perovskite or originally known as 2D Ruddlesden-Popper (RP) perovskite have a general formula of $A'_2A_{n-1}B_nX_{3n+1}$. The material transforms to layered material through adding organic separator between the layers of BX_6 octahedra with van der Waals force as the interlayer bond, resulting to the material being exfoliable to ultrathin layer.

5.1 Synthesis

Several methods can be used to synthesize layered perovskite as mentioned in section 4.1. To synthesize BA_2PbBr_4 (n=1) thin film, 2D RP perovskite formula must be satisfied, thus the molarity ratio of BA, MA, Pb, Br should be 2:0:1:4, as for n=2 and n=3, MA is included in both formulas making it $BA_2MAPb_2Br_7$ and $BA_2MA_2Pb_3Br_{10}$ therefore changing the molarity ratios.

Synthesizing thin film can be as straightforward as adding the ratios to solvent (DMF), then depositing the solution on the substrate on spin-coater as mentioned in section 4.1.1. But if the materials are not available in the lab, then the materials should be prepared using the following reactions:

$$PbBr2\text{: } 1\ mmol\ of\ PbO\ +\ 2\ mmol\ of\ HBr \rightarrow PbBr2\ +\ H2O$$

$$BABr\text{: } 2\ mmol\ of\ C_4H_9NH_2\ (butylamine)$$
$$+\ 2\ mmol\ of\ HBr \rightarrow 2C_4H_9NH_3Br\ (BABR)$$

The reaction leading to BABr is exothermic so it is recommended to prepare on ice bath to increase the rate of the reaction by slowing it down. Finally, slowly add $PbBr_2$ to 2BABr to get BA_2PbBr_4

5.2 Raman Spectra

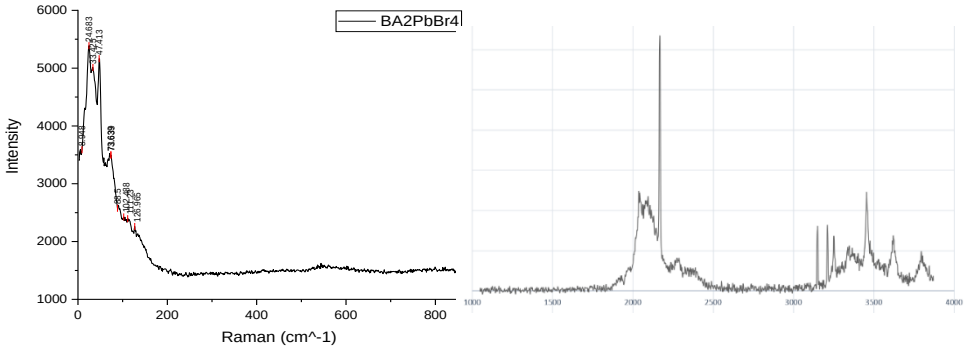

Figure 20. Left is low frequency Raman spectra with identified peaks. Right is High frequency Raman spectra. Taken with green laser at laser power of 200μW with 10 seconds of laser exposure.

Two Measurements have been taken for layered perovskite, the first measurement is high frequency (greater than 200 cm^{-1}) which shows the material fingerprint and other cases like defect and crystallinity. The second measurement is the low frequency which is sub 200 cm^{-1}, this measurement is taken when the material is layered, which shows the interatomic band between the layers. For perovskite, many peaks have been observed showing how complex the material is.

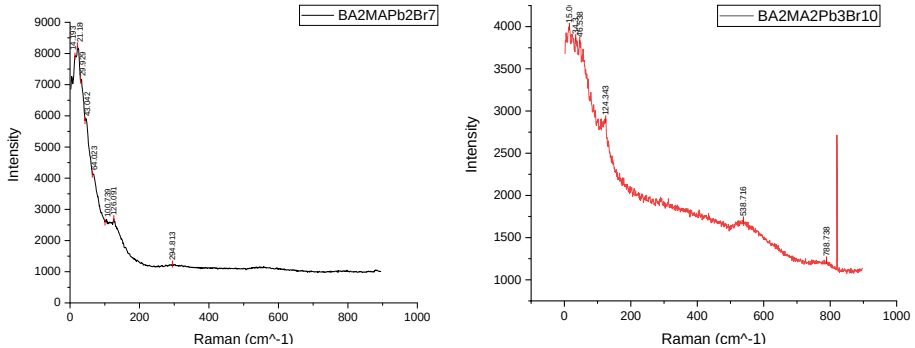

Figure 21. Left is Raman spectra of $BA_2MAPB_2Br_7$ and right is $BA_2MA_2Pb_3Br_{10}$ both with identified peaks. $BA_2MAPB_2Br_7$ Raman spectra is taken with green laser at laser power of (12) with 10 seconds of laser exposure and $BA_2MAPB_2Br_7$ is taken with green laser at laser

Small Raman shift have been observed when numbers of layers change, which shows that the interlayer bond have change at different layers numbers.

Changing the halogens (Cl, Br, I) changes the crystal structure due to halogens difference in bohr radius leading to a change in phonon dispersion thus changing the band structure. High frequency Raman shows a huge shift from ~2000 cm^{-1} to ~800 cm^{-1} when changing the halogens for bromine to iodine; this is evidence that phonon dispersion of the material has changed leading to a major change in the band structure (red shift in optical band gap from 3.1 eV to 2.4 eV as we will see in photoluminescence section 5.2.4. As for the low frequency Raman, the peaks in Iodine based layered perovskite are available in the Bromine based layered perovskite indicating that both have same layer numbers (n=1).

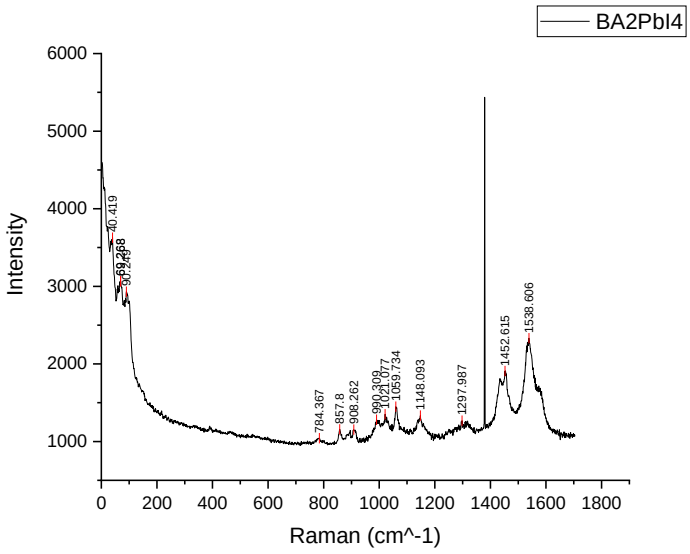

Figure 22. Left is PL of BA_2PbBr_4 showing a peak at 3.043 eV. Right is Comparison between different layers blue (n=1), green (n=2), red(n=3), black(n=∞). First three measurements were taken with UV laser power of 20mW with UV Filter embedded in the system.

5.3 X-Ray Diffraction

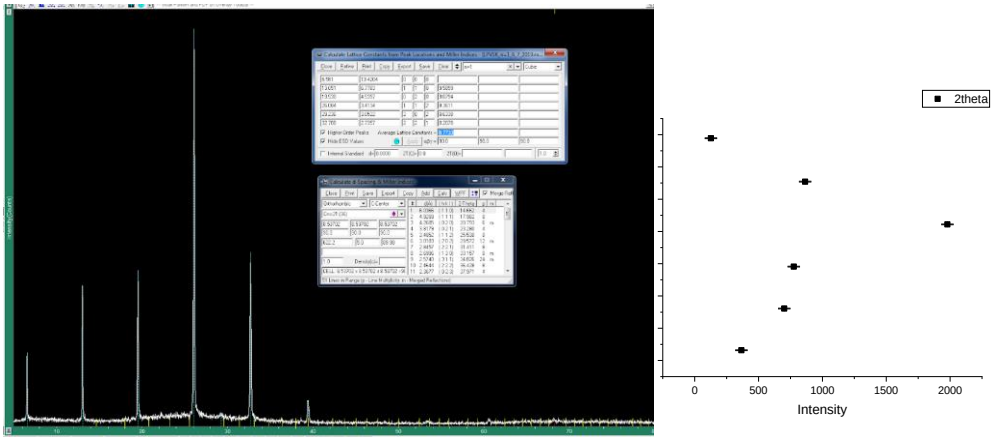

Figure 23. XRD spectrum of BA_2PbBr_4 measured using a wavelength of 0.2 nm. Right shows the average XRD peaks.

X-Ray Diffraction of layered perovskite at n=1 shows a parallel pattern which indicates that it is a layered material. As mentioned in section 1.3, the crystal structure of BA_2PbBr_4 at room temperature is orthorhombic while the space group at room temperature is Cmc2I according to Lekina's review article.[37] The X-Ray Diffraction spectrum shows high intensity peaks at 2θ= 6.56, 13.05, 19.54, 26.08 32.71 and 39.65. Atomic spacings analysed through Jade ranges from $1.34\dot{A} - 13\dot{A}$ and the average lattice constant has been calculated for b and c to be $\sim 8.77\ \dot{A}$ and a being 13 $\dot{A}$ hence it is an orthorhombic phase. XRD also shows sharp peaks with small width, which according to Scherrer's equation, means that the grain sizes are large.

5.4 Photoluminescence

Photoluminescence has been done to check the optical band gap of BA_2PbBr_4, $BA_2MAPb_2Br_7$, and $BA_2MA_2Pb_3Br_{10}$ showing optical band gaps of 3.037 eV, 2.81 eV and 2.697 eV respectively with at least 0.73 eV, 0.5 eV, and 0.39 eV differences from the bulk form of bromide perovskite (2.32 eV). It is observed that as n decreases, band gap increases, this means that the band gap can be easily tuned in the material giving a huge advantage for band gap engineering.

Band gap changing due to nanometer thickness variation is a quantum phenomenon called quantum confinement, where n – the number of ultrathin layers before adding a spacer – represents the thickness of the material. Both electron and hole energies increase as the thickness decrease due to the confinement of their waves at low nano scale hence their energies becomes quantized and changes with the relationship of E $\propto \frac{1}{t^2}$, therefore $E_{QC} = E_{gap} + E_e + E_h$, hence as the thickness decreases the band gap increases. Another phenomenon that appears strongly is the exciton binding energy as the perovskite changed from bulk to layered. The electronic band gap of BA_2PbBr_4 was proven to be 3.42 eV, hence the binding energy is ~383 meV.[41]

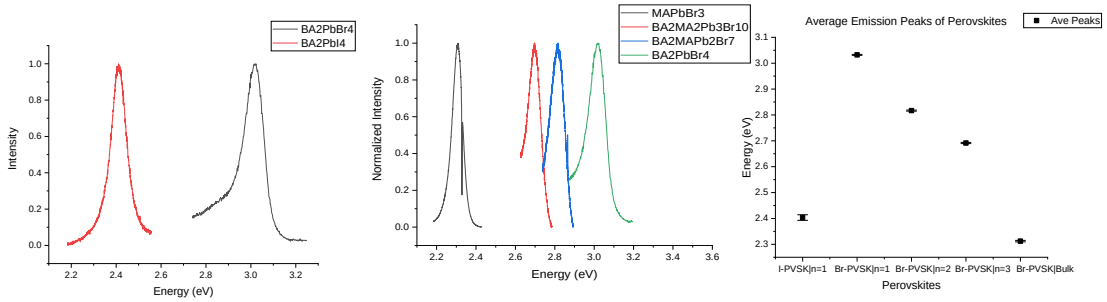

Figure 24. Left is Comparison of emission peaks between Bromide and Iodide based Perovskite. Middle shows comparison between different layers – blue (n=1), green (n=2), red(n=3), black(n=∞), and right is the average PL peaks.

Changing halogens also shifts the energy of the material because the band structure of the perovskite originates from the metal-halogen hybridization. The PL in Figure 15. shows energy change from 2.41 eV to 3.04 eV when changing iodine to bromine. The huge shift in energy is from the bohr radius of halogens decreasing when switching from iodine lighter halogens therefore decreasing the interatomic spacing between metal and halogen as a result the band gap increases. As for the binding energy of iodide-perovskite n=1, the band gap measured by Hong *et. al.* is 2.58 eV while the PL measurement shows a peak at 2.423 eV resulting in an exciton binding energy of ~147 meV.[42]

5.4.1 Temperature-Dependent PL

TDPL of Br-based and I-based layered perovskites (n=1) are measured and shown in Figure 26 and 27. Br-based layered perovskite shows the opposite effect of bulk perovskite (5.1.4.1), BA_2PbBr_4 shows red shift by 7 meV as temperature decreases that means that the effect of phonon frequency is larger than the thermal expansion interaction. TDPL also showed two phase transitions at ~240 C and ~150 C which are changes in crystal structure from orthorhombic I to orthorhombic II and orthorhombic II to tetragonal respectively.

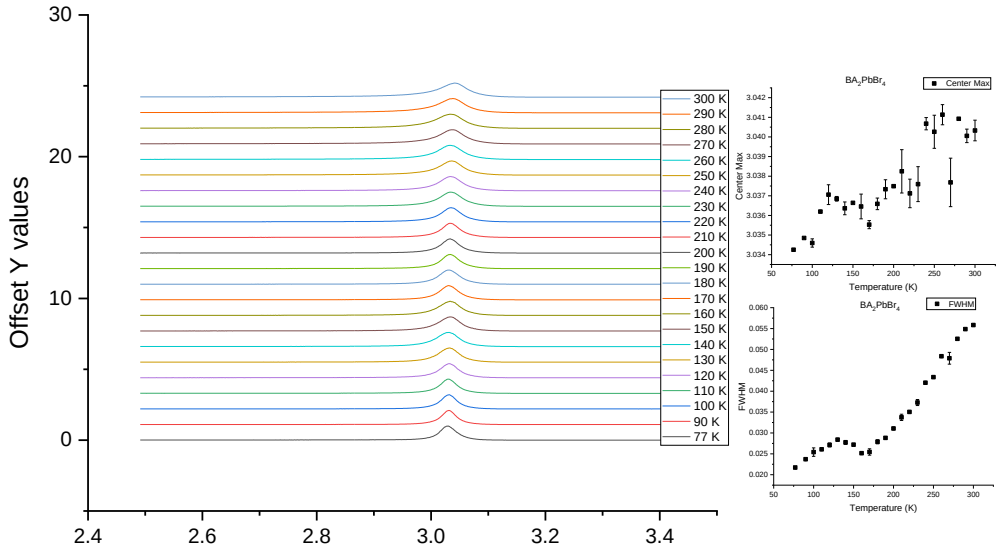

Figure 25. Left is TDPL of BA_2PbBr_4 and right is peak shift with temperature and FWHM.

Peaks have been analyzed at low-temperature (77 K) to find excitonic states, at the measured temperature there have been no indication of trions or biexcitons. A study has found biexciton photoluminescence of BA_2PbBr_4 at 3.015 eV when measured optical absorption spectra at 5K.[60]

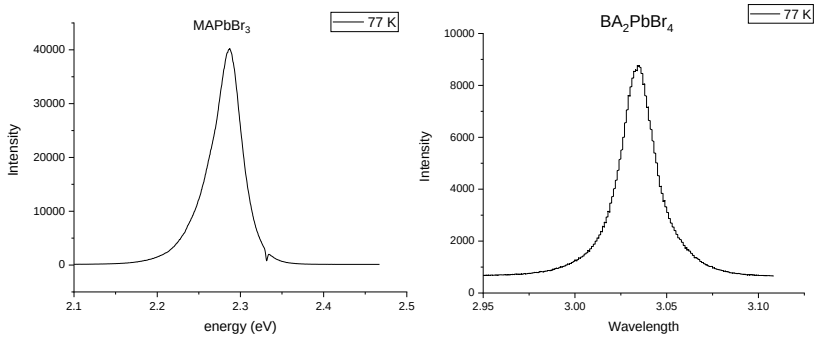

Figure 26. PL of BA_2PbBr_4 and $MAPbBr_3$ at 77 K.

5.4.2 Time-Resolved PL

TRPL measurement has been taken to compare between the different thicknesses n=1, 2, 3 and ∞ thin films which resulted in lifetimes of 50 ns, 0.375 μs, and > 0.4 μs respectively. This shows that lifetime shows a strong thickness dependence for hybrid perovskite and that lifetime shortens as thickness decreases, in fact the thickness effect the material so much that n=2 has ten times lifetime of n=1.

The superlattice structure of n=1 of having a dielectric layer after every semiconducting layer increasing the recombination rate making it a great radiating device. On the other hand, as the number of semiconducting layers increases before adding the spacer greatly increases the conductivity, making it a suitable photovoltaic device.

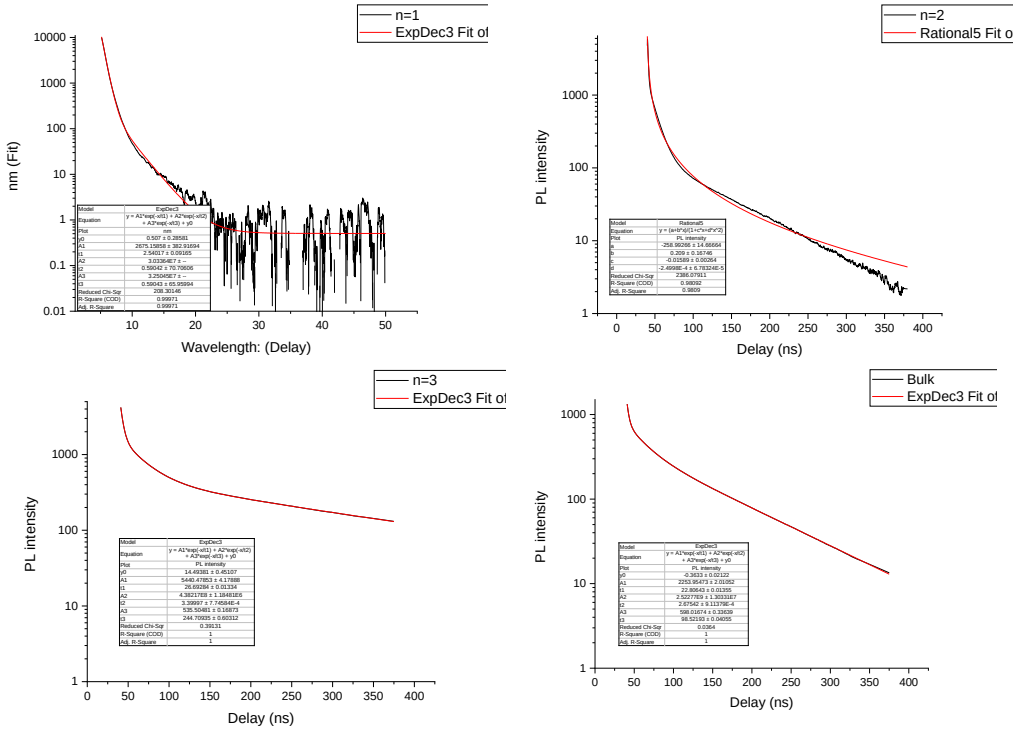

Figure 27. TRPL of different numbers of layers bromide perovskite.

5.5 Ultrathin: Perovskites and MoS_2

5.5.1 Synthesis:

5.5.1.1 Perovskites Monolayer (n=1 and 2)

Both layered perovskite crystals are prepared with the help of Tongay's team member Ying Qin who is specialized in chemistry. For n=1 crystal, 280 mg of PbO is mixed in 2.15 mL HBr and 0.425 mL H_3PO_2 in the first sample glass, resulting in $PbBr_2$, $2H_2O$, and PO. On another sample glass, an exothermic reaction between butylamine (BA) and HBR will take place so it is recommended to put the sample glass on ice bath then add 124 μL BA and 1.075 mL HBr ending with BABr and H_2. Then slowly add BABr to the $PbBr_2$ to instantly get BA_2PbBr_4 crystal. Layered perovskite with n=2 follows similar procedure accept with changing the concentration of PbO to 279 mg and adding 70 mg of MABr then mixing it with 2.15 mL of HBr in the first beaker, on the second beaker again prepare ice bath and mix 87 μL with 1.075 mL of HBr resulting in $BA_2MAPb_2Br_7$ crystal.

The crystals prepared should be recrystallized to get higher crystal quality therefore it is recommended to regrow using a profile temperature. After the preparation, directly seal the sample from temperature induced pressure to change the vapor pressure of the H_2O hence prevent vaporization at 110 °C and put the sealed sample glass in a programmable furnace with adding the following temperature profile: 4 hours increase to 110 °C constant at 110°C for 2 hours, 4 hours of cooling to 50 °C 16 hours of further cooling to 25 °C and finally 4 hours constant at 25 °C For the mechanical exfoliation, carefully dry the crystal with kim wipe then use the scotch tape. Place a bit of the bulk on folded ends tape then exfoliate several times on different regions of the tape trying to

cover as much area as possible, then cut another piece of the tape and place it on first tape, and same thing with the exfoliation trying to cover as much as possible.

After exfoliation, take a clean silicon/silicon dioxide substrate and place it on the exfoliated region of the tape and place your finger on the substrate for several seconds to increase adhesion between the monolayer and the substrate. Check for monolayers using light microscopy, it should be seen in Si/SiO_2 substrate, but nearly invisible when using silicon substrate due to poor contrast of the silicon. When the presence of monolayer is confirmed, place a clean silicon substrate on the same tape but different place using your finger for heat assistive adhesion.

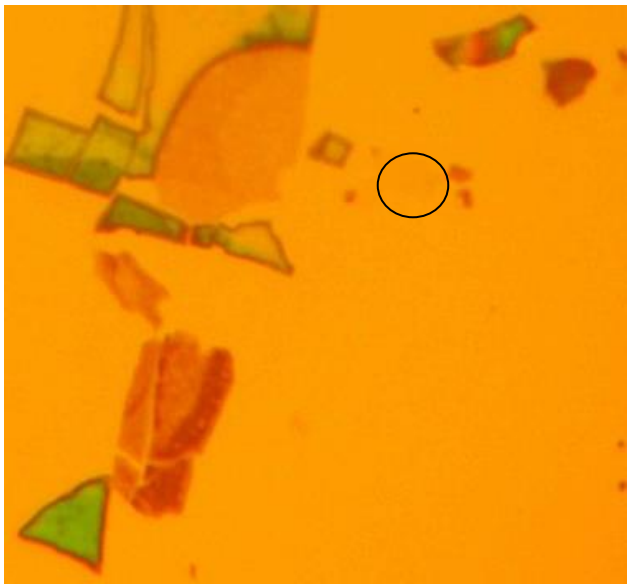

Figure 28. Image of MA_2PbBr_4 on silicon substrate under Light Microscopy, circled is monolayer.

5.5.1.2 MoS_2 Monolayer

TMD is one of the 2D families that bares semiconducting characteristics. Being a layered material with van der Waals interlayer bonding and great electrical and mechanical properties, TMD family has been excessively research. One of the most researched material in TMDs is MoS_2 due to great robustness and electrical properties making it a great candidate for transistors

Mos_2 monolayer can be extracted via mechanical exfoliation or grown using chemical vapor deposition. For mechanical exfoliation the same method has been used as done for layered perovskites. As for the CVD, the setup must be clean to grow monolayers. MoS_2 monolayers was grown with the help of Tongay's team members Dipesh Trivadi and Guven Turgut who are specialized in CVD growth.

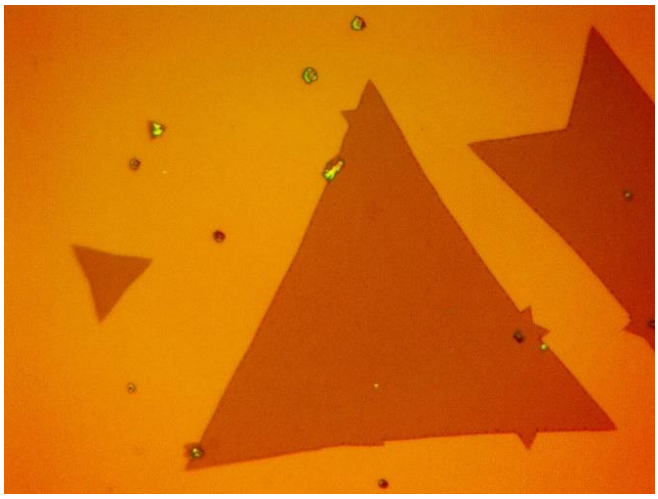

Figure 29. MoS_2 monolayer under light microscopy at 100x magnification.

5.3.2 AFM/KPFM

Thickness dependent Kelvin Probe Force Microscopy have been measured for BA_2PbBr_4, $BA_2MAPb_2Br_7$, and MoS_2 for several thicknesses. There has been a clear thickness dependence with surface potential for all measured materials. This characteristic will open a new opportunity of workfunction tuning using thickness in addition to doping.

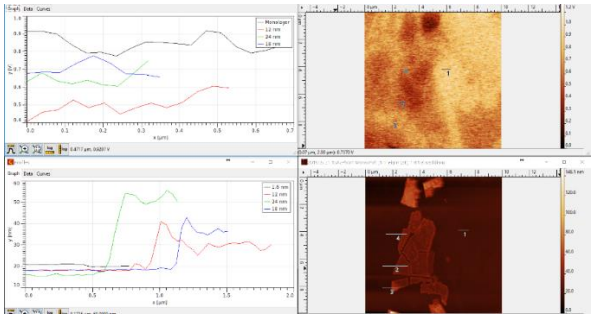

Figure 30. Top and bottom left are KPFM and bottom is AFM of $BA_2MAPb_2Br_7$

MoS_2 shows a huge surface potential difference for each additional layer, difference between n=1 and n=2 is 0.119 V and from n=1 and n=3 is 0.267 V while the surface potential difference between thicknesses 20 nm and 36 nm is a mere 0.022 V suggests that the relation between thickness of both MoS_2 and n=2 materials and surface potential is exponential as for n=1, the relation shown is linear.

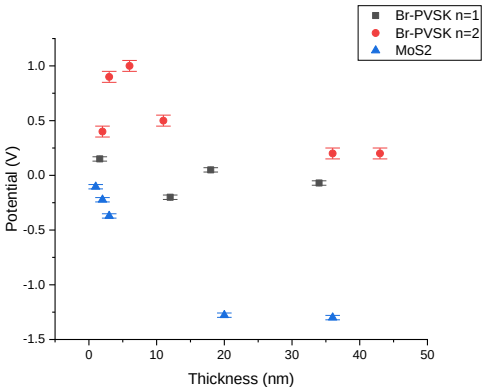

Figure 31. Thickness dependence KPFM of BA_2PbBr_4(squares), $BA_2MAPb_2Br_7$(circles), and MoS_2(triangles) monolayers

6 CONCLUSION AND FUTURE OPPORTUNITES

Organic-Inorganic Hybrid Perovskite is a direct band gap semiconductor that has been excessively studied for its strong application on optoelectronic devices including solar cells and LED. The structure of the material is cubic in room temperature with ABX_3 structure where A represents a large monocation, B is a small dication, and X is a halide. A layered form of perovskite was discovered which changed many properties of the material, the structure changes by adding an organic spacer between n numbers of layers. What makes layered perovskites interesting is the possibility of controlling the number of layers n before adding the spacer, which effects different perovskites properties.

A Fundamental study of bulk, layered, and monolayers bromide lead perovskites structural, optical, and electrical properties have been studied. As thickness changes, crystal structure changes from cubic to orthorhombic from bulk to layered, XRD and Raman spectrum show how the difference in the thicknesses change the crystal structures through observing changes in average lattice constant, atomic spacing, and lattice vibrations of the materials. XRD shows that perovskite has changed from its cubic phase, to orthorhombic phase when change the material to superlattice. It also shows that layered material has patterned peaks meaning that for each layer there is a spacer hence the layer number of the material is n=1.

Optical properties also have been studied mainly focusing on the thickness effect of different properties where the PL of n=1,2,3 and ∞ show emission energy shift from 2.33 eV to 3.04 eV and exciton binding energies increased to 360 meV as thickness of the material decreases due to the dielectric effect. Temperature dependent PL has

shown different characteristics when comparing $MAPbBr_3$ to BA_2PbBr_4, and when comparing the two different halides at a layer thickness of n=1 (BA_2PbBr_4 and BA_2PbI_4). TRPL displays different recombination lifetimes as thickness of bromide-based perovskite changes, it shows that lifetime significantly increases with increasing layer thicknesses resulting to a direct increase in the conductivity of the material, thicker layers are more suitable for photovoltaic device. Finally, this thesis introduced the thickness dependence KPFM of BA_2PbBr_4, $BA_2MAPb_2Br_7$, and MoS_2. The thicknesses started from monolayers ranging to tens of nms. It has been shown that the relation between thickness and surface potential has exponential relation, where the surface potential starts increasing exponentially as thickness reaches 20 nm for MoS_2 and 40 nm for perovskite, and increases more at sub-ten nm.

More Fundamental studies must be done to further examine these great materials, including more thoroughly study on different excitons for different materials, more investigation on instabilities in lead and tin halide perovskites, understanding more quantum effects including quantum dots and high-temperature superconductivity. Also, new perovskite families should be studied more extensively including new small metal cations, new organic cations and all inorganic perovskites.

REFERENCES

1. Zhang, W., Eperon, G. E. & Snaith, H. J. Metal halide perovskites for energy applications. *Nature Energy*1,(2016).

2. Perovskite Solar Cells. *Energy.gov*Available at: https://www.energy.gov/eere/solar/perovskite-solar-cells.

3. Oku, T. *et al.*Fabrication and Characterization of Element-Doped Perovskite Solar Cells. *Nanostructured Solar Cells*(2017). doi:10.5772/65768

4. Saliba, M. *et al.*How to Make over 20% Efficient Perovskite Solar Cells in Regular (n–i–p) and Inverted (p–i–n) Architectures. *Chemistry of Materials*30,4193–4201 (2018).

5. Elumalai, N., Mahmud, M., Wang, D. & Uddin, A. Perovskite Solar Cells: Progress and Advancements. *Energies*9,861 (2016).

6. Chen, Y. *et al.*2D Ruddlesden–Popper Perovskites for Optoelectronics - Chen - 2018 - Advanced Materials - Wiley Online Library. *Advanced Materials*(2017). Available at: https://www.onlinelibrary.wiley.com/doi/full/10.1002/adma.201703487.

7. Stoumpos, C. C. *et al.*Ruddlesden–Popper Hybrid Lead Iodide Perovskite 2D Homologous Semiconductors. *Chemistry of Materials*28,2852–2867 (2016).

8. Gangadharan, D. T. *et al.*Aromatic Alkylammonium Spacer Cations for Efficient Two-Dimensional Perovskite Solar Cells with Enhanced Moisture and Thermal Stability. *Solar RRL*2,1700215 (2018).

9. Nguyen, N.-T. Fabrication Technologies. *Micromixers*79–134 (2008). doi:10.1016/b978-081551543-2.50007-x

10. Spin Coating: A Guide to Theory and Techniques. *Ossila*Available at: https://www.ossila.com/pages/spin-coating.

11. Konstantakou, M., Perganti, D., Falaras, P. & Stergiopoulos, T. Anti-Solvent Crystallization Strategies for Highly Efficient Perovskite Solar Cells. *Crystals*7,291 (2017).

12. Jang, D. M., Kim, D. H., Lee, J. W. & Song, J. K. Ultrasound synthesis of lead halide perovskite nanocrystals. *Journal of Materials Chemistry C*(2016). Available at: https://pubs.rsc.org/en/content/articlelanding/2016/tc/c6tc04213a#!

13. Meng, L., You, J. & Yang, Y. Addressing the stability issue of perovskite solar cells for commercial applications. *Nature Communications*9,(2018).

14. Wan-Jian Yin, J.-H. Y., Kang, J. & Yanfa Yan, S.-H. W. Halide perovskite materials for solar cells: a theoretical review. *Journal of Materials Chemistry A*(2014). Available at: https://pubs.rsc.org/en/content/articlelanding/2015/ta/c4ta05033a#!

15. Ono, L. K., Juarez-Perez, E. J. & Qi, Y. Progress on Perovskite Materials and Solar Cells with Mixed Cations and Halide Anions. *ACS Applied Materials & Interfaces*9,30197–30246 (2017).

16. Bakulin, A. A. *et al.*Real-Time Observation of Organic Cation Reorientation in Methylammonium Lead Iodide Perovskites. *Real-Time Observation of Organic Cation Reorientation in Methylammonium Lead Iodide Perovskites | The Journal of Physical Chemistry Letters*(2015). Available at: http://pubs.acs.org/doi/abs/10.1021/acs.jpclett.5b01555.

17. Tanaka, K. *et al.*Electronic and Excitonic Structures of Inorganic–Organic Perovskite-Type Quantum-Well Crystal (C4H9NH3)2PbBr4. *Japanese Journal of Applied Physics***44,**5923–5932 (2005).

18. Niu, G. *et al.*Study on the stability of CH3NH3PbI3films and the effect of post-modification by aluminum oxide in all-solid-state hybrid solar cells. *J. Mater. Chem. A*2,705–710 (2014).

19. Aristidou, N. *et al.*The Role of Oxygen in the Degradation of Methylammonium Lead Trihalide Perovskite Photoactive Layers. *Angewandte Chemie International Edition*54,8208–8212 (2015).

20. Conings, B. *et al.*Intrinsic Thermal Instability of Methylammonium Lead Trihalide Perovskite. *Advanced Energy Materials*5,1500477 (2015).

21. Balandin, A. A. *et al.*Superior Thermal Conductivity of Single-Layer Graphene. *Nano Letters*8,902–907 (2008).

22. Novoselov, K. S. *et al.*Two-dimensional gas of massless Dirac fermions in graphene. *Nature News*(2005). Available at: https://www.nature.com/articles/nature04233.

23. Lee, C., Wei, X., Kysar, J. W. & Hone, J. Measurement of the Elastic Properties and Intrinsic Strength of Monolayer Graphene. *Science*321,385–388 (2008).

24. Nair, R. R. *et al.*Fine Structure Constant Defines Visual Transparency of Graphene. *Science*320,1308–1308 (2008).

25. Zhu, Y. *et al.*Graphene and Graphene Oxide: Synthesis, Properties, and Applications - Zhu - 2010 - Advanced Materials - Wiley Online Library. *Advanced Materials*(2010). Available at: https://onlinelibrary.wiley.com/doi/abs/10.1002/adma.201001068.

26. Miró, P., Audiffred, M. & Heine, T. An atlas of two-dimensional materials. *Chemical Society Reviews*(2014). doi:10.1039/C4CS00102H

27. Zhang, H. Ultrathin Two-Dimensional Nanomaterials. *ACS Nano*9,9451–9469 (2015).

28. Chiba, T. *et al.*Anion-exchange red perovskite quantum dots with ammonium iodine salts for highly efficient light-emitting devices. *Nature Photonics*12,681–687 (2018).

29. Wei, Z. High Performance Perovskite Light-Emitting Diodes with External Quantum Efficiency Exceeding 20% Achieved via Compositional Distribution Management. *The International Photonics and Optoelectronics Meeting (POEM)*(2018). doi:10.1364/pfe.2018.pf1b.3

30. Cao, Y. *et al.*Perovskite light-emitting diodes based on spontaneously formed submicrometre-scale structures. *Nature*562,249–253 (2018).

31. Kumawat, N. K. *Blue perovskite light-emitting diodes: progress, challenges and future directions*(2019). doi:10.1039/C8NR09885A

32 Fang, Y., Dong, Q., Shao, Y., Yuan, Y. & Huang, J. Highly narrowband perovskite single-crystal photodetectors enabled by surface-charge recombination. *Nature Photonics*9,679–686 (2015).

33 Akriti, Shi, E. & Dou, L. A Leap towards High-Performance 2D Perovskite Photodetectors. *Trends in Chemistry*1,365–367 (2019).

33. Cohen, B.-E., Wierzbowska, M. & Etgar, L. High efficiency quasi 2D lead bromide perovskite solar cells using various barrier molecules. *Sustainable Energy & Fuels***1,**1935–1943 (2017).

34. Genck, W. Make The Most of Antisolvent Crystallization. *Chemical Processing*(2010). Available at: https://www.chemicalprocessing.com/articles/2010/210/.

35. Time-Resolved Photoluminescence and Photovoltaics . in *Time-Resolved Photoluminescence and Photovoltaics* (National Renewable Energy Laboratory, 2005).

36. Castelli, I. E., García-Lastra, J. M., Thygesen, K. S. & Jacobsen, K. W. Bandgap calculations and trends of organometal halide perovskites. *APL Materials*2,081514 (2014).

37. Lekina, Y. & Shen, Z. X. Excitonic states and structural stability in two-dimensional hybrid organic-inorganic perovskites. *Journal of Science: Advanced Materials and Devices*(2019).

38. Melitz, W., Shen, J., Kummela, A. C. & Lee, S. Kelvin probe force microscopy and its application. *Surface Science Reports***66,**1–27 (2010).

39. Wang, K.-H., Li, L.-C., Shellaiah , M. & Sun , K. W. Structural and Photophysical Properties of Methylammonium Lead Tribromide (MAPbBr3) Single Crystals. *Nature Scientific Reports*(2017). doi:https://doi.org/10.1038/s41598-017-13571-1

40. Miyata, K., Atallah, T. L. & Zhu, X.-Y. Lead halide perovskites: Crystal-liquid duality, phonon glass electron crystals, and large polaron formation. *Science Advances*3,(2017).

41. Takagi, H., Kunugita, H. & Ema, K. Influence of the image charge effect on excitonic energy structure in organic-inorganic multiple quantum well crystals. *Physical Review B***87,**(2013).

42. Hong, X., Ishihara, T. & Nurmikko, A. V. Dielectric confinement effect on excitons inPbI4-based layered semiconductors. *Physical Review B*45,6961–6964 (1992).

F1. Walsh, A. Principles of Chemical Bonding and Band Gap Engineering in Hybrid Organic–Inorganic Halide Perovskites. *The Journal of Physical Chemistry C*119,5755–5760 (2015).

F2. Shi, Z. & Jayatissa, A. Perovskites-Based Solar Cells: A Review of Recent Progress, Materials and Processing Methods. *Materials*11,729 (2018).

F3. Feng, J. & Xiao, B. Crystal Structures, Optical Properties, and Effective Mass Tensors of CH3NH3PbX3 (X = I and Br) Phases Predicted from HSE06. *The Journal of Physical Chemistry Letters*5,1278–1282 (2014).

F4. Fan, Z., Sun, K. & Wang, J. Perovskites for photovoltaics: a combined review of organic–inorganic halide perovskites and ferroelectric oxide perovskites. *Journal of Materials Chemistry A*3,18809–18828 (2015).

F5. Leguy, A. M. A. *et al.*Dynamic disorder, phonon lifetimes, and the assignment of modes to the vibrational spectra of methylammonium lead halide perovskites. *Physical Chemistry Chemical Physics*18,27051–27066 (2016).

F6. Wang, B., Xiao, X. & Chen, T. Perovskite photovoltaics: a high-efficiency newcomer to the solar cell family. *Nanoscale*6,12287–12297 (2014).

F7. Huo, C., Cai, B., Yuan, Z., Ma, B. & Zeng, H. Two-Dimensional Metal Halide Perovskites: Theory, Synthesis, and Optoelectronics - Huo - 2017 - Small Methods - Wiley Online Library. *Small Methods*(2017). Available at: https://onlinelibrary.wiley.com/doi/abs/10.1002/smtd.201600018. (Accessed: 5th July 2019)

F8. Tongay's Research Lab

F9. Tongay, S. *Fundamental of Electrical, Magnetic, Optical Materials and Device Applications*

F10. Bruker D8 multipurpose Powder X-ray Diffractometer in ASU- PSC-B3

F11. Wang, C. X-Ray Characterization. *Semiconductor Characterization*

F12. AR Coating Techniques: Thin Film Deposition Methods. *FindLight Blog*(2017). Available at: https://www.findlight.net/blog/2017/12/15/ar-coating-techniques/.

F13. Yacoot, A. & Koenders, L. Aspects of scanning force microscope probes and their effects on dimensional measurement. *Journal of Physics D: Applied Physics***41,**103001 (2008).

F14. Wang, S. *et al.*Temperature-Dependent Band Gap in Two-Dimensional Perovskites: Thermal Expansion Interaction and Electron–Phonon Interaction. *The Journal of Physical Chemistry Letters***10,**2546–2553 (2019).

F15.Chemical Vapor Deposition - Nanoscience & Nanotechnology. *Google Sites* Available at: https://sites.google.com/site/nanomodern/Home/CNT/syncnt/cvd.

F16.Arizona State University - Engineering Wings